

Mono- W Dark Matter Signals at the LHC: Simplified Model Analysis

Nicole F. Bell, Yi Cai and Rebecca K. Leane

ARC Centre of Excellence for Particle Physics at the Terascale
School of Physics, The University of Melbourne, Victoria 3010, Australia

E-mail: n.bell@unimelb.edu.au, yi.cai@unimelb.edu.au,
rlean@physics.unimelb.edu.au

Abstract. We study mono- W signals of dark matter (DM) production at the LHC, in the context of gauge invariant renormalizable models. We analyze two simplified models, one involving an s -channel Z' mediator and the other a t -channel colored scalar mediator, and consider examples in which the DM-quark couplings are either isospin conserving or isospin violating after electroweak symmetry breaking. While previous work on mono- W signals have focused on isospin violating EFTs, obtaining very strong limits, we find that isospin violating effects are small once such physics is embedded into a gauge invariant simplified model. We thus find that the 8 TeV mono- W results are much less constraining than those arising from mono-jet searches. Considering both the leptonic (mono-lepton) and hadronic (mono fat jet) decays of the W , we determine the 14 TeV LHC reach of the mono- W searches with 3000 fb^{-1} of data. While a mono- W signal would provide an important complement to a mono-jet discovery channel, existing constraints on these models imply it will be a challenging signal to observe at the 14 TeV LHC.

Contents

1	Introduction	1
2	Simplified Models for the Mono-W	3
2.1	t -channel Colored Scalar Mediator	3
2.2	s -channel Z' Mediator	3
3	LHC Constraints and Reach	4
3.1	Mono lepton channel	4
3.2	Mono fat jet channel	6
3.3	Results	7
4	$SU(2)$ Breaking Effects and Enhancements from W_L Production	9
4.1	Isospin Violation in the t -channel Model	9
4.1.1	Cross Section Enhancement from W_L Contribution	10
4.1.2	$SU(2)$ Breaking and the M_T Spectrum	11
4.2	Isospin Violating Effects in s -channel Models	12
5	Conclusion	12
6	Acknowledgements	13

1 Introduction

Since dark matter (DM) was first suggested over 80 years ago, compelling evidence has accumulated for its existence across cosmological scales. However, the details of the fundamental particle properties of dark matter remain elusive. There exist a plethora of models which provide possible DM candidates, among which a particularly attractive and well-motivated class is weakly interacting massive particles (WIMPs) [1, 2].

The exact details of WIMP interactions with Standard Model (SM) particles are unknown, and it is thus convenient to describe these interactions in a model-independent manner. This is often done within an effective field theory (EFT) framework, in which the high energy renormalizable interactions are approximated at low energy by a set of non-renormalizable operators [3–5]. This low energy description is obtained from the full high-energy theory by integrating out heavy degrees of freedom. For fermionic dark matter, χ , interacting with SM fermions, f , the EFT operators take the form:

$$\frac{1}{\Lambda^2} (\bar{\chi}\Gamma_{\chi\chi}) (\bar{f}\Gamma_{ff}), \quad (1.1)$$

where the remnants of the high energy theory are encapsulated by the parameter Λ , which contains the mass M of the mediator and its couplings g_i in the form $\Lambda = M/\sqrt{g_1 g_2}$, and by $\Gamma_{\chi,f}$, which are the Lorentz structures of the interaction.

These EFT operators have found wide application in the LHC mono- X searches for DM production [4, 6–32]. These are generic search channels in which a visible SM final state recoils against the missing momentum carried off by a pair of DM particles. Typically

the mono-jet channel provides the most stringent constraints, while mono- W , Z , γ or Higgs signals would provide indispensable complementary information to identify DM.

The EFT approximation is valid when the momentum transfer in a given process of interest is much smaller than the mass of the mediating particle. For momentum transfer larger than or comparable to Λ , the EFT description will break down. This situation is likely to arise at the LHC, where the momentum of the partons in the colliding protons, and thus the momentum transfer of the scattering processes, will be of TeV scale and comparable to Λ in many WIMP scenarios. The precise values of the parameters for which this break down occurs have been the subject of several recent papers [33–36]. An alternative framework which avoids these issues is “simplified models” [37–42]. In this framework a mediator is explicitly included and interaction types which are generic yet phenomenologically distinct are considered.

However, the validity of the EFT description is not governed only by the size of Λ . The standard list of EFT operators [3, 4] include several which do not respect the weak gauge symmetries of the SM¹. Such operators break down at the energies comparable to the electroweak scale, $v_{\text{EW}} \approx 246$ GeV, rather than the energy scale of new physics, Λ , and are certainly invalid at LHC energies. In fact, such operators should be suppressed by powers of $(v_{\text{EW}}/\Lambda)^n$, and are thus of higher order in $1/\Lambda$ than they naively appear. One should proceed with caution in interpreting LHC limits on such operators.

In a recent paper [43] we demonstrated that operators which violate weak gauge symmetries can feature spurious cross section enhancements at LHC energies. This was particularly pertinent for previous mono- W searches for dark matter at the LHC [8, 10, 15], which have largely focused on $SU(2)$ violating EFTs such as [22]

$$\frac{1}{\Lambda^2} (\bar{\chi}\gamma^\mu\chi) (\bar{u}\gamma_\mu u + \xi\bar{d}\gamma_\mu d), \quad (1.2)$$

with $\xi \neq 1$. The large mono- W cross sections for such an EFT are in fact a manifestation of the violation of weak gauge invariance in the form of unphysical longitudinal W contributions. Previous work has used these unphysical enhancements of the mono- W cross section to place very strong limits on dark matter EFTs. However, when gauge invariance is enforced we shall see that the limits arising from the mono- W process will in general be weaker than those arising from the mono-jet. Nonetheless, the mono- W process remains an important complementary channel to explore the properties of dark matter.

It is the purpose of the present paper to study mono- W signals in renormalizable models in which gauge invariance is enforced from the outset. We choose two example simplified models, one involving t -channel exchange of a new colored scalar, and the other s -channel exchange of a new Z' vector boson. We outline these two models in Section 2. In Section 3 we explore the LHC phenomenology of these models, to determine the current constraints and the 14 TeV LHC reach for the mono- W signal. In Section 4 we explore the possibility of obtaining $SU(2)$ violating operators, like that of Eq. (1.2), from a gauge invariant model after electroweak symmetry breaking. While such operators would allow for the production of longitudinal W_L bosons, potentially enhancing mono- W cross sections, we explain why these effects are constrained to be small.

¹Indeed, some simplified models also have this shortcoming.

2 Simplified Models for the Mono- W

2.1 t -channel Colored Scalar Mediator

We first examine a scenario in which DM-quark interactions are mediated by the exchange of a t -channel scalar. The interaction Lagrangian is given by

$$\begin{aligned}\mathcal{L}_{\text{int}} &= f\bar{Q}_L\eta\chi_R + h.c. \\ &= f_{ud}(\eta_u\bar{u}_L + \eta_d\bar{d}_L)\chi_R + h.c.,\end{aligned}\tag{2.1}$$

where $Q_L = (u_L, d_L)^T$ is the quark doublet, $\eta = (\eta_u, \eta_d)^T \sim (3, 2, 1/6)$ is a scalar field that transforms under the SM gauge group like Q_L , and f is the coupling strength of the interactions². The DM, χ , transforms as a singlet under the SM gauge symmetries. An analogue of this scenario is realized in supersymmetric (SUSY) models, where we identify η with a squark doublet and χ the neutralino. Simplified models with such t -channel interactions have been examined recently in Refs. [46–52], with the collider analyses focusing on the mono-jet process.

In this model, the mono- W process proceeds via the gauge invariant set of diagrams in Fig. (1) [21, 43, 53, 54]. Diagrams (1a) and (1b) dominate in the EFT limit when $\sqrt{s} \ll m_\eta$, while diagram (1c) becomes important for smaller m_η . We shall initially assume $m_{\eta_u} = m_{\eta_d} = m_\eta$. Deviation from this equality will be discussed in Section 4.

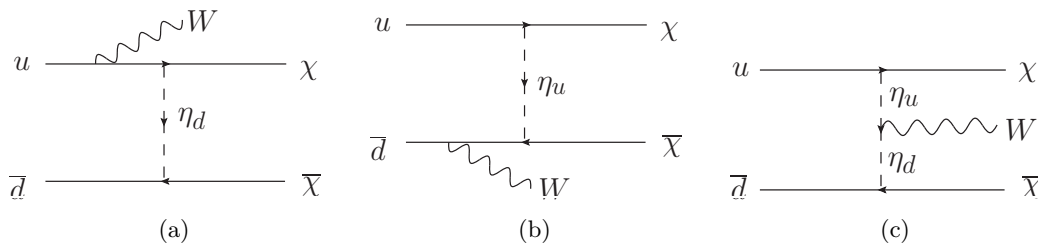


Figure 1. Contributions to the mono- W process $u(p_1)\bar{d}(p_2) \rightarrow \chi(k_1)\bar{\chi}(k_2)W^+(q)$, in a t -channel colored scalar model.

2.2 s -channel Z' Mediator

We also consider another generic simplified model in which the DM-quark interactions are mediated by a neutral spin-1 Z' boson. The relevant interaction terms are

$$\mathcal{L}_{\text{int}} \supset g_\chi\bar{\chi}\gamma^\mu\gamma^5\chi Z'_\mu + g_q\bar{q}\gamma^\mu\gamma^5q Z'_\mu,\tag{2.2}$$

where g_χ is the coupling strength of the Z' to dark matter χ , and g_q is the coupling to SM quarks. Simplified models with such s -channel interactions have been examined recently in Refs. [55–71]. We assume the Z' has axial vector type interactions. Vector interactions would lead to large spin-independent DM-nucleon elastic scattering cross sections, and as a result are strongly constrained by DM direct detection experiments, to the extent that parameters which can correctly account for the DM relic density are significantly excluded.

²One can write down a similar model involving a coupling to right handed (RH) quark fields. While most of the phenomenology would be very similar, such a model would not permit a mono- W signal. Isospin violating models with RH quark fields were considered in [44, 45].

We therefore focus on the more phenomenologically viable axial vector interactions. We shall also assume that the Z' couples only to quarks, and not to leptons, to avoid tight constraints from di-lepton searches.

The pertinent processes for mono- W search are shown in Fig. (2). In contrast to the t -channel model above, no radiation from the mediator occurs. This would change in the presence of Z - Z' mixing, as will be discussed in Section 4.

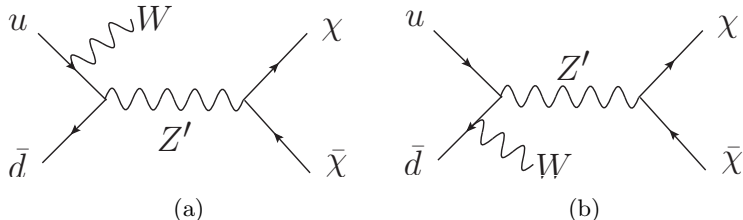


Figure 2. Contributions to the mono- W process $u(p_1)\bar{d}(p_2) \rightarrow \chi(k_1)\bar{\chi}(k_2)W^+(q)$, in an s -channel Z' model.

3 LHC Constraints and Reach

We now examine the LHC phenomenology of the two models described in Eqs. (2.1) and (2.2). In the following, we determine the limits and reach of the searches for DM via the mono- W process, for both the leptonic and hadronic decay channels of the W .

3.1 Mono lepton channel

We first consider the scenario where the W boson decays to a charged lepton and a neutrino. The neutrino contributes to the missing energy (\cancel{E}_T) along with dark matter, such that the signal is a mono-lepton. In this channel the key kinematic variable is the transverse mass of the lepton- \cancel{E}_T system,

$$M_T = \sqrt{2p_T^\ell \cancel{E}_T (1 - \cos \Delta\phi_{\ell, \cancel{E}_T})}, \quad (3.1)$$

where $\Delta\phi_{\ell, \cancel{E}_T}$ is the azimuthal opening angle between the charged lepton's transverse momentum p_T and the direction of \cancel{E}_T .

The dominant background for the mono-lepton search is $W \rightarrow \ell\nu$, and $W \rightarrow \tau\nu_\tau \rightarrow \nu_\tau\nu_\tau\ell\nu_\ell$ where $\ell = e, \mu$. This is because the M_T distribution of these channels has a large tail in the signal region. We use the electron channel to set limits, since it is the stronger one of two lepton channels and also comparable to the combined limits of both channels. Following Ref. [15], the following selection cuts are made on all backgrounds and signal for the 8 TeV limits:

- E_T of the leading electron > 100 GeV
- E_T of the next-to-leading electron < 35 GeV
- At least one electron
- M_T for the electron, $M_T^e > 220$ GeV
- Pseudorapidity for the electron must be in the range $-2.1 < \eta(\ell_e) < 2.1$

- Jet $P_T < 45$ GeV
- The electron P_T and \cancel{E}_T ratio must be in the range $0.4 < P_T/\cancel{E}_T < 1.5$
- $\Delta\phi_{e,\cancel{E}_T} > 2.5$.

After cuts, the events are scaled by the relevant efficiencies. To investigate the phenomenology, both models are implemented in FEYNRULES [72]. For the mono-lepton search, events are generated in MADGRAPH/MADEVENT [73, 74], hadronized in PYTHIA [75], interfaced with FASTJET [76] for jet-finding and DELPHES [77] for detector effects. We then implement our cuts in ROOT [78], and set the model significance σ at 95 % confidence level (C.L.), which is set by the number of signal events S and background events B as

$$\sigma = \frac{S}{\sqrt{S + B + (\delta B * B)^2}}, \quad (3.2)$$

where δB is the systematic uncertainty, which we take to be 5% for our analysis. To ensure a thorough sampling of events and sufficient statistics at high M_T , we generate event samples at two different regions for both signal and background, $100 < p_T^\ell < 500$ GeV, and $p_T^\ell > 500$ GeV. The samples from these two regions are then combined to produce the background and signal events. We find that we reproduce the model independent limit on the cross section for a mono-lepton signal as found in Ref. [15], at 8 TeV. We then perform the analysis at 14 TeV and $3000 fb^{-1}$ integrated luminosity. To produce our 95% C.L. reach, we optimize our 14 TeV selection criteria by increasing the M_T cut to $M_T^e > 1000$ GeV. In Fig. (3) we show the M_T distribution for the t -channel model for various choices of the DM mass. (Similar results are found for the s -channel model.) As the shape of the M_T distribution is approximately independent of the DM mass, we adopt $M_T > 1000$ GeV as an optimal selection cut across all parameter choices.

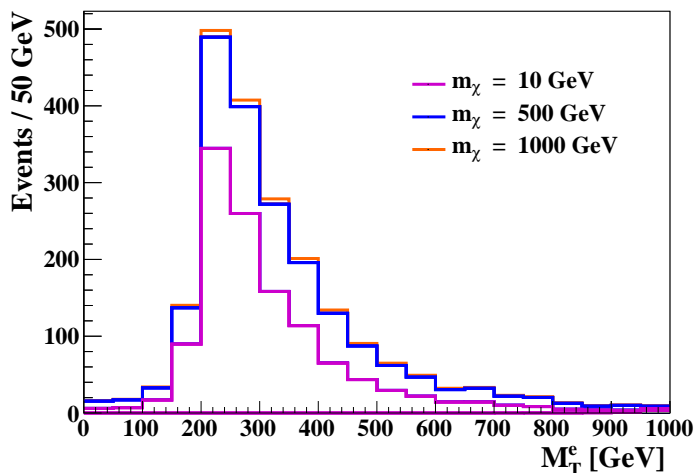


Figure 3. M_T distribution for $m_{\eta_u} = m_{\eta_d} = 200$ GeV, $g = 1$, $m_\chi = 10, 500, 1000$ GeV in the t -channel model, at 14 TeV and $\mathcal{L}_{int} = 3000 fb^{-1}$. It can be seen that the distribution is independent of DM mass.

3.2 Mono fat jet channel

We also consider the limits and reach from the hadronic W decays. Such decays have been searched for by ATLAS [10], where the signal is a hadronically decaying W or Z boson plus missing energy. As our simplified models allow both mono- W and mono- Z processes, both must be included in our generated signal. We refer to this channel as the “mono fat jet” channel as the hadronic decay products jj of the W/Z can be strongly boosted such that they appear together as one wide jet, making the signal this “fat jet” along with \cancel{E}_T from DM.

The relevant backgrounds for this search are $Z \rightarrow \nu\bar{\nu}$, $W \rightarrow \ell^\pm\nu$, $Z \rightarrow \ell\ell$, WW , WZ , ZZ , $t\bar{t}$ and top production. We generate backgrounds in HERWIG++ [79], where events are also hadronized. Using both our models implemented in FEYNRULES [72], signal events are generated in MADGRAPH/MADEVENT [73, 74] and are hadronized in PYTHIA [75]. Both signal and background events are then passed to external FASTJET [76], where we implement jet finding algorithms and cuts, followed by DELPHES [77] for detector effects and efficiencies. Specifically, in order to discriminate between background jets and those produced by the W/Z , a mass-drop filtering procedure is used. Here, large radius jet candidates which mostly come from the decay of the W/Z are first reconstructed via the Cambridge-Aachen algorithm [80] with a radius parameter of 1.2. Then, the internal structure of this large radius jet is examined, and the subjets, called “narrow jets”, are reconstructed using the anti-kt jet clustering algorithm [81] with a radius parameter of 0.4. The mass-drop is performed on the two leading subjets, where the subjet with the largest p_T , p_{T1} differs from the momentum of the next to leading subjet p_{T2} by

$$\sqrt{y} = \min(p_{T1}, p_{T2}) \frac{\Delta R}{m_{jet}}, \quad (3.3)$$

where ΔR is the separation of the two leading subjets and m_{jet} is the mass of the large radius jet. For 8 TeV, following the analysis of [10], we also require:

- $\cancel{E}_T > 350$ GeV
- At least one large radius jet with $P_T > 250$ GeV
- $\sqrt{y} > 0.4$
- $50 < m_{jet} < 120$ GeV
- $-1.2 < \eta < 1.2$
- No more than one narrow jet with $P_T > 40$ GeV and $-4.5 < \eta < 4.5$ which is separated from the leading large radius jet as $\Delta R > 0.9$
- $\Delta\phi(jet, \cancel{E}_T) < 0.4$ for narrow jets.

As the $Z \rightarrow \nu\nu$ background process in this channel has low statistics after cuts, to ensure a thorough probe of phase space we generate and average 6 sets of 50,000 events at 14 TeV for this background. For the other background processes, we generate 50,000 events per process. We set the model significance at 95 % C.L. , as per Eq. (3.2). For the 14 TeV reach, we optimize the search by adjusting three of the 8 TeV selection criteria; we now require at least one large radius jet with $P_T > 400$ GeV, require $\cancel{E}_T > 500$ GeV and $70 < m_{jet} < 90$ GeV.

3.3 Results

For the t -channel model, the current limits are compared with the 14 TeV mono- W reach in Fig. (4) for $f_{u,d} = 1$. We also include current constraints on the parameter space from mono-jet and multi-jet searches, which are adopted from Ref. [47]. The region labelled “stability” is forbidden as it corresponds to parameters where $m_\chi > m_\eta$ and thus the DM would be unstable to decay. For the mono-lepton search, we find that both the current 8 TeV exclusion and 14 TeV reach are not competitive with existing constraints from mono-jet searches. Owing to small signal size and large backgrounds, it is too weakly constraining to be featured on our t -channel summary plot. For the mono fat jet search, we find that the 8 TeV exclusions are also not competitive with existing constraints from mono-jet searches. We show the 14 TeV reach in the mono fat jet channel with 3000 fb^{-1} of data, which is able to probe a region of parameter space unconstrained by existing mono-jet results.

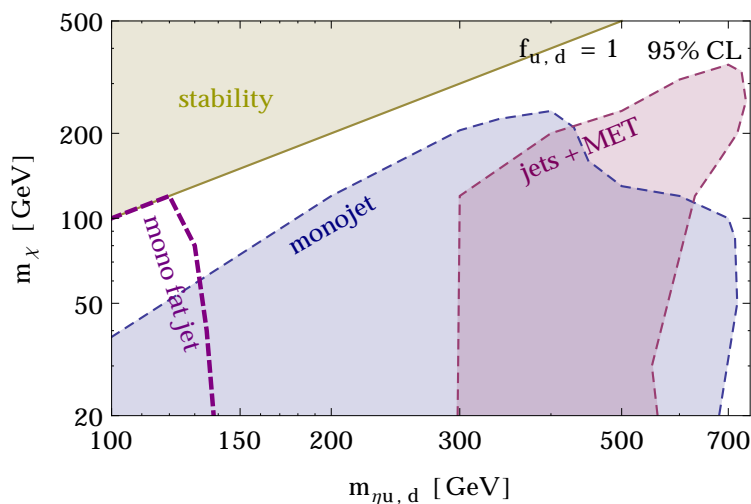
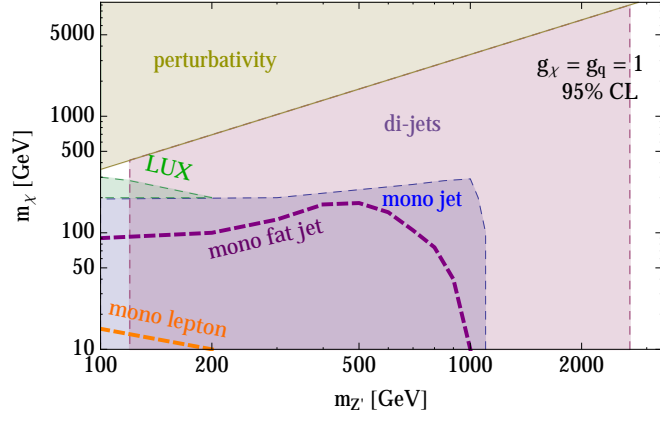


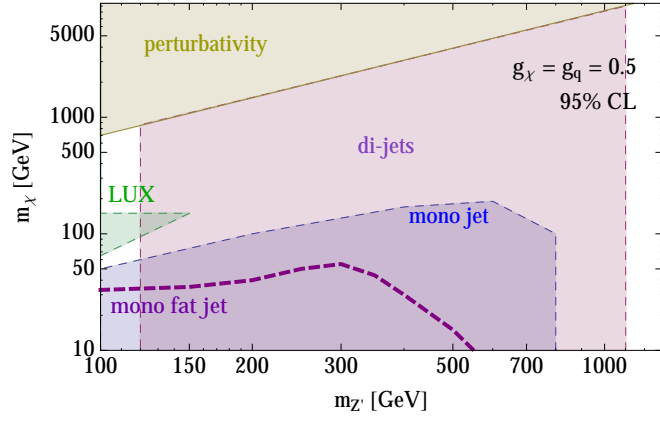
Figure 4. Parameter space for the t -channel colored scalar model, for $f_{u,d} = 1$. Exclusions are shown as shaded regions for the mono and multi jet at 8 TeV, and the reach is shown for the mono fat jet at 14 TeV 3000 fb^{-1} .

For the s -channel model, our results are shown in Fig. (5) for three choices of the Z' couplings to DM and quarks, as labelled. The relevant mono-jet, di-jet and LUX [82] direct detection limits shown are adopted from Ref. [83]. Note that the LUX limit assumes the actual (sub-critical) contribution to the DM relic density implied by the model parameters, rather than assuming a full relic density. We also include perturbativity limits for the s -channel model. As has been recently shown in [83, 84], the s -channel model with axial couplings may have perturbativity and unitarity issues without the inclusion of additional new physics such a dark Higgs scalar which generates the DM and Z' mass. Perturbative unitarity implies that the Z' cannot be much lighter than the DM, and should satisfy $m_\chi \lesssim \frac{\sqrt{4\pi}}{g_\chi} m_{Z'}$. This is shown on the s -channel plots as the perturbativity region. While this is not a concrete exclusion, it is an important issue for this region of parameter space.

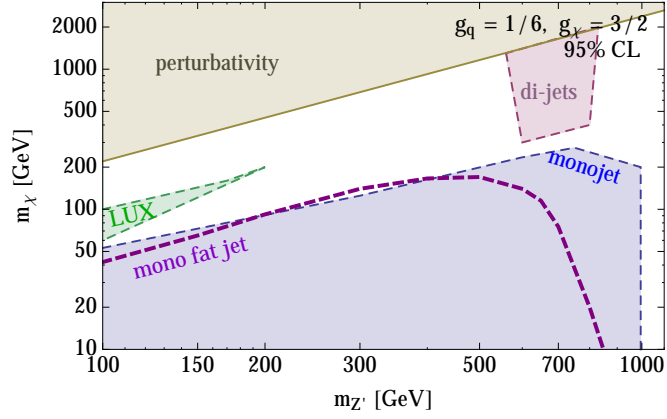
For the mono-lepton search, the current 8 TeV exclusion is too weak to be shown on the plots, while the 14 TeV reach is shown only for $g_q = g_\chi = 1$, as it is very weakly constraining for the other coupling choices. As with the t -channel model, the mono fat jet channel has better sensitivity than the mono-lepton channel, and the 14 TeV reach is shown for each of the



(a)



(b)



(c)

Figure 5. Parameter space for the s -channel Z' model, for choices of (a) $g_q = g_\chi = 1$ and (b) $g_q = g_\chi = 0.5$ and (c) $g_q = 1/6$ and $g_\chi = 3/2$. Exclusions are shown as shaded regions for LUX and for mono-jet and di-jets at 8 TeV, and the reaches are shown for the mono lepton ((a) only) and mono fat jet searches at 14 TeV $3000 fb^{-1}$. Note differing axes.

coupling choices. However, even with the hadronic decay mode, the mono- W signals will be challenging to observe, with the parameter space accessible at 14 TeV already substantially probed by 8 TeV mono-jet searches.

4 $SU(2)$ Breaking Effects and Enhancements from W_L Production

Previous work on the mono- W signal has focused primarily on EFT operators that violate $SU(2)_L$. The strong constraints on these models were shown to arise from unphysical high-energy contributions from longitudinally polarized W bosons, a manifestation of the lack of gauge invariance [43]. The strength of the limits on these W_L dominated processes arose from two effects:

- enhancement of the cross section, due to a leading s/m_W^2 dependence for large s (arising from the W_L contribution to the polarization sum) [43] and
- a harder M_T distribution [15], which allowed better separation of signal and background.

By contrast, the gauge invariant simplified models that we considered above, which feature only transverse W_T contributions in the high energy limit, do not benefit from these effects. However $SU(2)$ violating effects, such as the unequal coupling of DM to u and d type quarks of Eq. (1.2), can be generated at higher order by electroweak symmetry breaking. This would permit some high energy W_L contributions to the mono- W process, potentially leading to stronger constraints. We analyze the size of such effects in variations of our simplified models, and show that it is always small.

4.1 Isospin Violation in the t -channel Model

In the t -channel model, the DM interaction with the u and d quarks can be of unequal strength if the masses of the respective mediators, η_u and η_d , are non-degenerate. Inspection of the scalar potential reveals that this situation can be realised once the SM Higgs field gains a vev. The scalar potential is [85]

$$V = m_1^2(\Phi^\dagger\Phi) + \frac{1}{2}\lambda_1(\Phi^\dagger\Phi)^2 + m_2^2(\eta^\dagger\eta) + \frac{1}{2}\lambda_2(\eta^\dagger\eta)^2 + \lambda_3(\Phi^\dagger\Phi)(\eta^\dagger\eta) + \lambda_4(\Phi^\dagger\eta)(\eta^\dagger\Phi), \quad (4.1)$$

where Φ is the SM Higgs and λ_n are coupling constants. In the case where $m_1^2 < 0$ and $m_2^2 > 0$, the SM Higgs doublet obtains a vev, while η does not. After electroweak symmetry breaking, a non-zero value of λ_4 would split the η masses as

$$m_{\eta_d}^2 = m_2^2 + (\lambda_3 + \lambda_4)v_{EW}^2, \quad (4.2)$$

$$m_{\eta_u}^2 = m_2^2 + \lambda_3v_{EW}^2, \quad (4.3)$$

so that

$$\delta m_\eta^2 \equiv m_{\eta_d}^2 - m_{\eta_u}^2 = \lambda_4 v_{EW}^2. \quad (4.4)$$

So we appear to have broken the degeneracy of the DM interactions with u and d type quarks, as in the EFT of Eq. (1.2). Does this indeed allow for W_L production, and how can this be understood?

It is instructive to appeal to the Goldstone boson equivalence theorem to understand where W_L production arises. In the high energy limit, we may replace W_L with the corresponding Goldstone boson that (in unitary gauge) provides the gauge boson mass, i.e., we replace W_L^+ with ϕ^+ . Now consider the 3 diagrams contributing to the mono- W process shown in Fig. (1). The ϕ^+ couples to the quarks with strength given by the quark Yukawa constants, which vanish in the limit that the quarks are massless. Under these conditions, there is no W_L contributions from the diagrams of Fig. (1a) and (1b).

We now turn to the diagram of Fig. (1c) in which the W is radiated from the η mediator. In general, this diagram will feature both W_T and W_L contributions. From inspection of the λ_4 term in Eq. (4.1), we deduce that ϕ^+ will couple to η according to [85]

$$v_{EW} \lambda_4 \eta_d \eta_u^* \phi^+ + h.c., \quad (4.5)$$

and thus the size of the $\eta_d \eta_u^* W_L^+$ vertex is determined by λ_4 . Therefore, switching on $\lambda_4 \neq 0$ and hence $\delta m_\eta^2 \neq 0$ opens a $pp \rightarrow \chi\chi W_L$ channel that does not suffer from suppression by the quark Yukawas. (By contrast, in the example studied in Section 3 where $\lambda_4 = 0$ and $\delta m_\eta^2 = 0$, we expect that the high energy regime will feature only transversely polarized W -bosons, $pp \rightarrow \chi\chi W_T$.)

4.1.1 Cross Section Enhancement from W_L Contribution

We have seen that the amplitude for W_L production at high energy is controlled by λ_4 . However, λ_4 also increases the mass splitting, making η_d heavier than η_u . Therefore, increasing λ_4 will suppress the contribution of Fig. (1a) due to the heavier η_d propagator, while enhancing the contribution of Fig. (1c) due to W_L production. The former effect dominates for small values of λ_4 , while the latter compensates or dominates if λ_4 is sufficiently large.

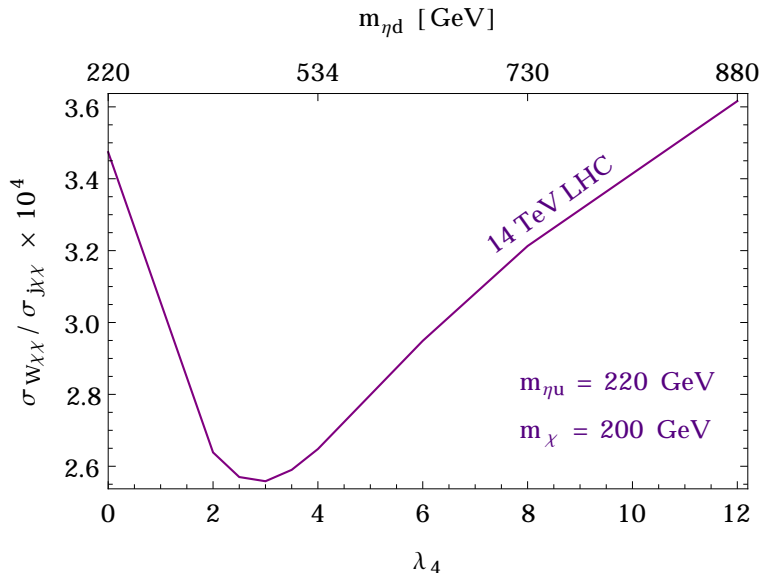


Figure 6. Ratio of the hadron level cross sections for the mono- W process $pp \rightarrow \chi\bar{\chi}W$, $\sigma_{W\chi\chi}$, to the mono-jet process $pp \rightarrow \chi\chi j$, $\sigma_{j\chi\chi}$ at 14 TeV, in a renormalizable t -channel scalar model with isospin violation. Upon increasing the mass splitting, the cross section decreases at first due to suppression from an increased propagator mass, until the longitudinal W contribution begins to dominate. The mono-jet cross section is monotonically decreasing with increase in propagator mass.

In Fig. (6) we show the ratio of the cross sections for the mono- W and mono-jet processes at hadron level at the 14 TeV LHC, as a function of λ_4 . (Although we have illustrated this behavior for a particular choice of the χ and η_u masses, we obtain similar behavior for other parameter choices.) While the mono-jet cross section monotonically decreases as λ_4 is increased, caused by the heavier η_d propagator, the mono- W cross section first decreases and then increases again when radiation of W_L from the η propagator takes over. However, in order to achieve a significant enhancement of the ratio of the mono- W to mono-jet cross sections, very large values of λ_4 are required. If we restrict this parameter to perturbative values, $\lambda_4 < 4\pi$, a relative enhancement cannot be achieved.

This behavior differs greatly to that seen in $SU(2)$ violating EFTs, where gauge non-invariant contributions from the analogue of Fig. (1 a,b) lead to large W_L contributions. In our renormalizable model, where all 3 diagrams of Fig. (1 a,b,c) are properly included, the high energy behavior of the cross section is tamed.

4.1.2 $SU(2)$ Breaking and the M_T Spectrum

We now consider the M_T distribution of the mono- W events. For the EFT model of Eq. (1.2), the mono- W M_T distributions were found to be sensitive to the parameter ξ [15]. Compared to the $SU(2)$ conserving choice $\xi = 1$, the $SU(2)$ breaking choice of $\xi \neq 1$ resulted in a harder M_T distribution, with a higher peak and significantly more high M_T events. This was useful in differentiating the signal from background via appropriate cuts on the minimum value of M_T .

To explore this effect in our t -channel simplified model, we plot the M_T distribution for various choices of λ_4 , shown in Fig. (7). We see that increasing the mass splitting parameter λ_4 produces no noticeable shift in the peak or shape of the M_T distribution. Therefore, the shape of the M_T distribution cannot be exploited to increase sensitivity.

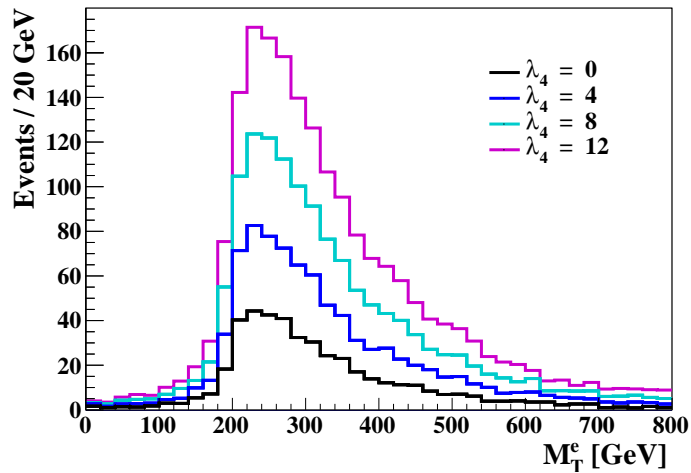


Figure 7. M_T distribution for $m_{\eta_u} = 220$ GeV, $g = 1$, $m_\chi = 200$ GeV in the t -channel model with isospin violation, at 14 TeV and $\mathcal{L}_{int} = 300 \text{ fb}^{-1}$. Despite the increase in λ_4 and therefore the mass splitting, the peak of the M_T distribution does not increase, leading to no strong advantage in the mono-lepton channel compared to other channels.

4.2 Isospin Violating Effects in s -channel Models

We now consider $SU(2)$ violating interactions of DM with quarks in the context of the s -channel Z' model. In the example model presented in Section 2, the Z' boson was taken to couple with equal strength to the u and d type quarks. This would be expected in a scenario in which the SM quarks were charged under the new $U(1)_{Z'}$. However, if the SM quarks were not charged under $U(1)_{Z'}$, and the Z' -quark couplings were to arise only via mixing of the Z' with the SM Z , then weak isospin violating interactions would result – see section A2 of Ref. [42]. In fact, these weak isospin violating interactions would be the lowest order DM-quark interaction terms present.

In the Z - Z' mixing scenario the quark- Z' couplings are proportional to the quark- Z couplings, which are of opposite sign for u and d quarks due to their weak isospin assignments of $T_3 = \pm 1/2$. In the EFT limit, where the Z' is integrated out, this would result in the operator of Eq. (1.2) with a negative value of ξ . However, the strength of the DM-quark interactions would be suppressed by the Z - Z' mixing angle, which is of order $v_{\text{EW}}^2/M_{Z'}^2$, and thus the operator arises only at order $1/\Lambda^4$. The relevant diagrams for the mono- W process are shown in Fig.(8). Unlike the Z' model of Section 2, there is now a diagram in which the W is radiated from the Z/Z' mediator. This diagram occurs at the same order in $1/\Lambda$ as the first two contributions³. While the third diagram will allow W_L production, the gauge invariance of the underlying theory prevents any bad high energy behavior, limiting any W_L driven cross section enhancement. Moreover, given that the Z - Z' mixing angle is constrained to be small, isospin violating effects will be difficult to observe.

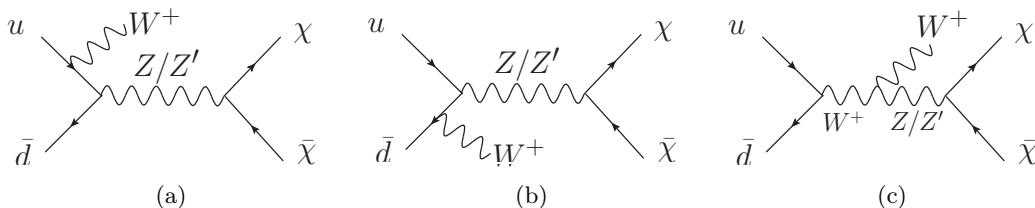


Figure 8. Contributions to the mono- W process $u(p_1)\bar{d}(p_2) \rightarrow \chi(k_1)\bar{\chi}(k_2)W^+(q)$, in the Z - Z' mixing model.

Finally, weak isospin violating effects would also occur in a model in which a new s -channel scalar mediator mixes with the SM Higgs. In this case the effects are suppressed by the small SM quark Yukawa couplings. In addition, if the DM is lighter than the Higgs, the Higgs invisible branching fraction would constrain the scalar-Higgs mixing.

5 Conclusion

Observation of DM production at the LHC is now one of the foremost goals of the particle physics community. To analyze the sensitivity of these searches, it is important to use a theoretically consistent framework for describing the DM interactions. The goal of this paper was to explore mono- W signals of dark matter production, in simplified models in which invariance under the SM weak gauge symmetries is enforced. We therefore considered popular

³If we included only the first two diagrams, e.g., by assuming only the operator of Eq. (1.2), we would encounter unphysical W_L effects whose origin could be traced to the lack of gauge invariance.

simplified models with an s -channel Z' mediator or a t -channel colored scalar mediator, both with and without isospin violating effects arising from electroweak symmetry breaking.

We first analyzed the simplified models in which the DM-quark couplings preserve isospin. Considering both the leptonic and hadronic decay modes of the W , we found that the 8 TeV mono- W sensitivity is not competitive with the 8 TeV mono-jet results. At 14 TeV the hadronic (mono fat jet) decay channel is the most promising, although 3000 fb^{-1} of data is required to significantly probe parameter space. While we anticipate that the experimental collaborations will be able to better optimize their analyses than the estimates we present here, we expect these general conclusions to hold.

Previous mono- W analyses have focused primarily on EFT operators that violate $SU(2)_L$, obtaining limits that are competitive with, or stronger than, those arising from the mono-jet. Therefore, we explored the possibility of obtaining isospin-violating DM-quark couplings in our gauge invariant simplified models, after electroweak symmetry breaking. This can be achieved in the t -channel model through the mass splitting of the squark-like scalar $SU(2)$ doublet, or in the s -channel model via Z - Z' mixing. For the both t -channel and s -channel models we find that these isospin violating effects must be small, in contrast to the non gauge invariant EFTs scenarios considered previously in the literature. As such, isospin violating DM-quark couplings are unlikely to increase the sensitivity of mono- W searches.

If DM is detected in future LHC data, it is likely that the mono-jet process will be the discovery channel. However, observation of a mono-jet signal alone would not be sufficient to elucidate the particular DM model. Complementary information from other channels such as the mono- W would eventually play an essential role. However, it will be challenging to observe these complementary signals at the 14 TeV LHC unless the model parameters fall just beyond the 8 TeV mono-jet reach. The observation of a mono- W signal at the 14 TeV LHC would therefore point toward very specific DM models. While mono- W signals can, in principle, probe isospin violation of the DM-quark couplings, encoding important information about the specific DM model, it may take a future collider for such effects to be observed.

6 Acknowledgements

N.F.B., Y.C. and R.K.L. were supported by the Australian Research Council. We acknowledge important discussions with T.J. Weiler and J.B. Dent, and thank Y. Bai for pointing out the Z - Z' mixing scenario of Section 4.2. Feynman diagrams are made using JAXODRAW [86].

References

- [1] L. Bergstrom, *Nonbaryonic dark matter: Observational evidence and detection methods*, *Rept. Prog. Phys.* **63** (2000) 793, [[hep-ph/0002126](#)].
- [2] G. Bertone, D. Hooper, and J. Silk, *Particle dark matter: Evidence, candidates and constraints*, *Phys. Rept.* **405** (2005) 279–390, [[hep-ph/0404175](#)].
- [3] J. Goodman, M. Ibe, A. Rajaraman, W. Shepherd, T. M. P. Tait, and H.-B. Yu, *Constraints on Light Majorana dark Matter from Colliders*, *Phys. Lett.* **B695** (2011) 185–188, [[arXiv:1005.1286](#)].
- [4] J. Goodman, M. Ibe, A. Rajaraman, W. Shepherd, T. M. P. Tait, and H.-B. Yu, *Constraints on Dark Matter from Colliders*, *Phys. Rev.* **D82** (2010) 116010, [[arXiv:1008.1783](#)].

- [5] M. Duch, B. Grzadkowski, and J. Wudka, *Classification of effective operators for interactions between the Standard Model and dark matter*, [arXiv:1412.0520](#).
- [6] **ATLAS** Collaboration, G. Aad et al., *Search for new phenomena in final states with an energetic jet and large missing transverse momentum in pp collisions at $\sqrt{s} = 8$ TeV with the ATLAS detector*, *Eur. Phys. J.* **C75** (2015), no. 7 299, [[arXiv:1502.01518](#)]. [Erratum: *Eur. Phys. J.*C75,no.9,408(2015)].
- [7] **ATLAS** Collaboration, G. Aad et al., *Search for new phenomena in events with a photon and missing transverse momentum in pp collisions at $\sqrt{s} = 8$ TeV with the ATLAS detector*, *Phys. Rev.* **D91** (2015), no. 1 012008, [[arXiv:1411.1559](#)]. [Erratum: *Phys. Rev.*D92,no.5,059903(2015)].
- [8] **ATLAS** Collaboration, G. Aad et al., *Search for new particles in events with one lepton and missing transverse momentum in pp collisions at $\sqrt{s} = 8$ TeV with the ATLAS detector*, *JHEP* **1409** (2014) 037, [[arXiv:1407.7494](#)].
- [9] **ATLAS** Collaboration, G. Aad et al., *Search for dark matter in events with a Z boson and missing transverse momentum in pp collisions at $\sqrt{s} = 8$ TeV with the ATLAS detector*, *Phys. Rev.* **D90** (2014), no. 1 012004, [[arXiv:1404.0051](#)].
- [10] **ATLAS** Collaboration, G. Aad et al., *Search for dark matter in events with a hadronically decaying W or Z boson and missing transverse momentum in pp collisions at $\sqrt{s} = 8$ TeV with the ATLAS detector*, *Phys.Rev.Lett.* **112** (2014), no. 4 041802, [[arXiv:1309.4017](#)].
- [11] **ATLAS** Collaboration, G. Aad et al., *Search for invisible particles produced in association with single-top-quarks in proton-proton collisions at $\sqrt{s} = 8$ TeV with the ATLAS detector*, *Eur. Phys. J.* **C75** (2015), no. 2 79, [[arXiv:1410.5404](#)].
- [12] **ATLAS** Collaboration, G. Aad et al., *Search for dark matter in events with heavy quarks and missing transverse momentum in pp collisions with the ATLAS detector*, *Eur. Phys. J.* **C75** (2015), no. 2 92, [[arXiv:1410.4031](#)].
- [13] **CMS** Collaboration, V. Khachatryan et al., *Search for dark matter, extra dimensions, and unparticles in monojet events in proton-proton collisions at $\sqrt{s} = 8$ TeV*, *Eur. Phys. J.* **C75** (2015), no. 5 235, [[arXiv:1408.3583](#)].
- [14] **CMS** Collaboration, V. Khachatryan et al., *Search for new phenomena in monophoton final states in proton-proton collisions at $\sqrt{s} = 8$ TeV*, [arXiv:1410.8812](#).
- [15] **CMS** Collaboration, V. Khachatryan et al., *Search for physics beyond the standard model in final states with a lepton and missing transverse energy in proton-proton collisions at $\sqrt{s} = 8$ TeV*, [arXiv:1408.2745](#).
- [16] **CMS** Collaboration, V. Khachatryan et al., *Search for Monotop Signatures in Proton-Proton Collisions at $\sqrt{s} = 8$ TeV*, *Phys. Rev. Lett.* **114** (2015), no. 10 101801, [[arXiv:1410.1149](#)].
- [17] **CMS** Collaboration, V. Khachatryan et al., *Search for the production of dark matter in association with top-quark pairs in the single-lepton final state in proton-proton collisions at $\sqrt{s} = 8$ TeV*, *JHEP* **06** (2015) 121, [[arXiv:1504.03198](#)].
- [18] L. M. Carpenter, A. Nelson, C. Shimmin, T. M. P. Tait, and D. Whiteson, *Collider searches for dark matter in events with a Z boson and missing energy*, *Phys. Rev.* **D87** (2013), no. 7 074005, [[arXiv:1212.3352](#)].
- [19] L. Carpenter, A. DiFranzo, M. Mulhearn, C. Shimmin, S. Tulin, and D. Whiteson, *Mono-Higgs-boson: A new collider probe of dark matter*, *Phys. Rev.* **D89** (2014), no. 7 075017, [[arXiv:1312.2592](#)].
- [20] A. A. Petrov and W. Shepherd, *Searching for dark matter at LHC with Mono-Higgs production*, *Phys. Lett.* **B730** (2014) 178–183, [[arXiv:1311.1511](#)].

- [21] N. F. Bell, J. B. Dent, A. J. Galea, T. D. Jacques, L. M. Krauss, and T. J. Weiler, *Searching for Dark Matter at the LHC with a Mono-Z*, *Phys. Rev.* **D86** (2012) 096011, [[arXiv:1209.0231](#)].
- [22] Y. Bai and T. M. Tait, *Searches with Mono-Leptons*, *Phys.Lett.* **B723** (2013) 384–387, [[arXiv:1208.4361](#)].
- [23] A. Birkedal, K. Matchev, and M. Perelstein, *Dark matter at colliders: A Model independent approach*, *Phys. Rev.* **D70** (2004) 077701, [[hep-ph/0403004](#)].
- [24] Y. Gershtein, F. Petriello, S. Quackenbush, and K. M. Zurek, *Discovering hidden sectors with mono-photon Z' searches*, *Phys. Rev.* **D78** (2008) 095002, [[arXiv:0809.2849](#)].
- [25] A. Crivellin, U. Haisch, and A. Hibbs, *LHC constraints on gauge boson couplings to dark matter*, *Phys. Rev.* **D91** (2015) 074028, [[arXiv:1501.00907](#)].
- [26] F. J. Petriello, S. Quackenbush, and K. M. Zurek, *The Invisible Z' at the CERN LHC*, *Phys. Rev.* **D77** (2008) 115020, [[arXiv:0803.4005](#)].
- [27] A. Berlin, T. Lin, and L.-T. Wang, *Mono-Higgs Detection of Dark Matter at the LHC*, *JHEP* **06** (2014) 078, [[arXiv:1402.7074](#)].
- [28] T. Lin, E. W. Kolb, and L.-T. Wang, *Probing dark matter couplings to top and bottom quarks at the LHC*, *Phys. Rev.* **D88** (2013), no. 6 063510, [[arXiv:1303.6638](#)].
- [29] P. J. Fox, R. Harnik, J. Kopp, and Y. Tsai, *Missing Energy Signatures of Dark Matter at the LHC*, *Phys. Rev.* **D85** (2012) 056011, [[arXiv:1109.4398](#)].
- [30] Y. Bai, J. Bourbeau, and T. Lin, *Dark matter searches with a mono-Z jet*, *JHEP* **06** (2015) 205, [[arXiv:1504.01395](#)].
- [31] M. Autran, K. Bauer, T. Lin, and D. Whiteson, *Searches for dark matter in events with a resonance and missing transverse energy*, *Phys. Rev.* **D92** (2015), no. 3 035007, [[arXiv:1504.01386](#)].
- [32] A. Gupta, R. Primulando, and P. Saraswat, *A New Probe of Dark Sector Dynamics at the LHC*, *JHEP* **09** (2015) 079, [[arXiv:1504.01385](#)].
- [33] G. Busoni, A. De Simone, E. Morgante, and A. Riotto, *On the Validity of the Effective Field Theory for Dark Matter Searches at the LHC*, *Phys.Lett.* **B728** (2014) 412–421, [[arXiv:1307.2253](#)].
- [34] G. Busoni, A. De Simone, J. Gramling, E. Morgante, and A. Riotto, *On the Validity of the Effective Field Theory for Dark Matter Searches at the LHC, Part II: Complete Analysis for the s-channel*, *JCAP* **1406** (2014) 060, [[arXiv:1402.1275](#)].
- [35] G. Busoni, A. De Simone, T. Jacques, E. Morgante, and A. Riotto, *On the Validity of the Effective Field Theory for Dark Matter Searches at the LHC Part III: Analysis for the t-channel*, *JCAP* **1409** (2014) 022, [[arXiv:1405.3101](#)].
- [36] O. Buchmuller, M. J. Dolan, and C. McCabe, *Beyond Effective Field Theory for Dark Matter Searches at the LHC*, *JHEP* **01** (2014) 025, [[arXiv:1308.6799](#)].
- [37] J. Abdallah, A. Ashkenazi, A. Boveia, G. Busoni, A. De Simone, et al., *Simplified Models for Dark Matter and Missing Energy Searches at the LHC*, [[arXiv:1409.2893](#)].
- [38] M. R. Buckley, D. Feld, and D. Goncalves, *Scalar Simplified Models for Dark Matter*, *Phys.Rev.* **D91** (2015) 015017, [[arXiv:1410.6497](#)].
- [39] **LHC New Physics Working Group** Collaboration, D. Alves et al., *Simplified Models for LHC New Physics Searches*, *J.Phys.* **G39** (2012) 105005, [[arXiv:1105.2838](#)].
- [40] J. Alwall, P. Schuster, and N. Toro, *Simplified Models for a First Characterization of New Physics at the LHC*, *Phys.Rev.* **D79** (2009) 075020, [[arXiv:0810.3921](#)].

- [41] J. Abdallah et al., *Simplified Models for Dark Matter Searches at the LHC*, *Phys. Dark Univ.* **9-10** (2015) 8–23, [[arXiv:1506.03116](#)].
- [42] D. Abercrombie et al., *Dark Matter Benchmark Models for Early LHC Run-2 Searches: Report of the ATLAS/CMS Dark Matter Forum*, [arXiv:1507.00966](#).
- [43] N. F. Bell, Y. Cai, J. B. Dent, R. K. Leane, and T. J. Weiler, *Dark matter at the LHC: Effective field theories and gauge invariance*, *Phys. Rev.* **D92** (2015), no. 5 053008, [[arXiv:1503.07874](#)].
- [44] J. L. Feng, J. Kumar, D. Marfatia, and D. Sanford, *Isospin-Violating Dark Matter*, *Phys. Lett.* **B703** (2011) 124–127, [[arXiv:1102.4331](#)].
- [45] J. L. Feng, J. Kumar, and D. Sanford, *Xenophobic Dark Matter*, *Phys.Rev.* **D88** (2013), no. 1 015021, [[arXiv:1306.2315](#)].
- [46] A. DiFranzo, K. I. Nagao, A. Rajaraman, and T. M. Tait, *Simplified models for dark matter interacting with quarks*, *JHEP* **1311** (2013) 014, [[arXiv:1308.2679](#)].
- [47] Y. Bai and J. Berger, *Fermion Portal Dark Matter*, *JHEP* **11** (2013) 171, [[arXiv:1308.0612](#)].
- [48] H. An, L.-T. Wang, and H. Zhang, *Dark matter with t -channel mediator: A simple step beyond contact interaction*, *Phys. Rev. D* **89** (2014) 115014, [[arXiv:1308.0592](#)].
- [49] S. Chang, R. Edezhath, J. Hutchinson, and M. Luty, *Effective WIMPs*, *Phys. Rev.* **D89** (2014), no. 1 015011, [[arXiv:1307.8120](#)].
- [50] M. Papucci, A. Vichi, and K. M. Zurek, *Monojet versus the rest of the world I: t -channel models*, *JHEP* **11** (2014) 024, [[arXiv:1402.2285](#)].
- [51] M. Garny, A. Ibarra, and S. Vogl, *Signatures of Majorana dark matter with t -channel mediators*, *Int. J. Mod. Phys.* **D24** (2015), no. 07 1530019, [[arXiv:1503.01500](#)].
- [52] M. Garny, A. Ibarra, S. Rydbeck, and S. Vogl, *Majorana Dark Matter with a Coloured Mediator: Collider vs Direct and Indirect Searches*, *JHEP* **06** (2014) 169, [[arXiv:1403.4634](#)].
- [53] N. F. Bell, J. B. Dent, A. J. Galea, T. D. Jacques, L. M. Krauss, and T. J. Weiler, *W/Z Bremsstrahlung as the Dominant Annihilation Channel for Dark Matter, Revisited*, *Phys. Lett.* **B706** (2011) 6–12, [[arXiv:1104.3823](#)].
- [54] P. Ciafaloni, M. Cirelli, D. Comelli, A. De Simone, A. Riotto, and A. Urbano, *On the Importance of Electroweak Corrections for Majorana Dark Matter Indirect Detection*, *JCAP* **1106** (2011) 018, [[arXiv:1104.2996](#)].
- [55] O. Buchmueller, M. J. Dolan, S. A. Malik, and C. McCabe, *Characterising dark matter searches at colliders and direct detection experiments: Vector mediators*, *JHEP* **01** (2015) 037, [[arXiv:1407.8257](#)].
- [56] J. Heisig, M. Krämer, M. Pellen, and C. Wiebusch, *Constraints on Majorana Dark Matter from the LHC and IceCube*, [arXiv:1509.07867](#).
- [57] D. Hooper, *Z' mediated dark matter models for the Galactic Center gamma-ray excess*, *Phys. Rev.* **D91** (2015) 035025, [[arXiv:1411.4079](#)].
- [58] M. Blennow, J. Herrero-Garcia, T. Schwetz, and S. Vogl, *Halo-independent tests of dark matter direct detection signals: local DM density, LHC, and thermal freeze-out*, *JCAP* **1508** (2015), no. 08 039, [[arXiv:1505.05710](#)].
- [59] O. Lebedev and Y. Mambrini, *Axial dark matter: The case for an invisible Z* , *Phys. Lett.* **B734** (2014) 350–353, [[arXiv:1403.4837](#)].
- [60] A. Alves, A. Berlin, S. Profumo, and F. S. Queiroz, *Dark Matter Complementarity and the Z' Portal*, *Phys. Rev.* **D92** (2015), no. 8 083004, [[arXiv:1501.03490](#)].
- [61] A. Alves, S. Profumo, and F. S. Queiroz, *The dark Z' portal: direct, indirect and collider searches*, *JHEP* **04** (2014) 063, [[arXiv:1312.5281](#)].

- [62] A. Alves, A. Berlin, S. Profumo, and F. S. Queiroz, *Dirac-fermionic dark matter in $U(1)_X$ models*, *JHEP* **10** (2015) 076, [[arXiv:1506.06767](#)].
- [63] H. An, X. Ji, and L.-T. Wang, *Light Dark Matter and Z' Dark Force at Colliders*, *JHEP* **07** (2012) 182, [[arXiv:1202.2894](#)].
- [64] H. An, R. Huo, and L.-T. Wang, *Searching for Low Mass Dark Portal at the LHC*, *Phys. Dark Univ.* **2** (2013) 50–57, [[arXiv:1212.2221](#)].
- [65] M. T. Frandsen, F. Kahlhoefer, A. Preston, S. Sarkar, and K. Schmidt-Hoberg, *LHC and Tevatron Bounds on the Dark Matter Direct Detection Cross-Section for Vector Mediators*, *JHEP* **07** (2012) 123, [[arXiv:1204.3839](#)].
- [66] G. Arcadi, Y. Mambrini, M. H. G. Tytgat, and B. Zaldivar, *Invisible Z' and dark matter: LHC vs LUX constraints*, *JHEP* **03** (2014) 134, [[arXiv:1401.0221](#)].
- [67] I. M. Shoemaker and L. Vecchi, *Unitarity and Monojet Bounds on Models for DAMA, CoGeNT, and CRESST-II*, *Phys. Rev.* **D86** (2012) 015023, [[arXiv:1112.5457](#)].
- [68] M. T. Frandsen, F. Kahlhoefer, S. Sarkar, and K. Schmidt-Hoberg, *Direct detection of dark matter in models with a light Z'* , *JHEP* **09** (2011) 128, [[arXiv:1107.2118](#)].
- [69] P. Gondolo, P. Ko, and Y. Omura, *Light dark matter in leptophobic Z' models*, *Phys. Rev.* **D85** (2012) 035022, [[arXiv:1106.0885](#)].
- [70] M. Fairbairn and J. Heal, *Complementarity of dark matter searches at resonance*, *Phys. Rev.* **D90** (2014), no. 11 115019, [[arXiv:1406.3288](#)].
- [71] P. Harris, V. V. Khoze, M. Spannowsky, and C. Williams, *Constraining Dark Sectors at Colliders: Beyond the Effective Theory Approach*, *Phys. Rev.* **D91** (2015) 055009, [[arXiv:1411.0535](#)].
- [72] C. Degrande, C. Duhr, B. Fuks, D. Grellscheid, O. Mattelaer, and T. Reiter, *UFO - The Universal FeynRules Output*, *Comput. Phys. Commun.* **183** (2012) 1201–1214, [[arXiv:1108.2040](#)].
- [73] J. Alwall, M. Herquet, F. Maltoni, O. Mattelaer, and T. Stelzer, *MadGraph 5 : Going Beyond*, *JHEP* **06** (2011) 128, [[arXiv:1106.0522](#)].
- [74] F. Maltoni and T. Stelzer, *MadEvent: Automatic event generation with MadGraph*, *JHEP* **02** (2003) 027, [[hep-ph/0208156](#)].
- [75] T. Sjostrand, S. Mrenna, and P. Z. Skands, *PYTHIA 6.4 Physics and Manual*, *JHEP* **05** (2006) 026, [[hep-ph/0603175](#)].
- [76] M. Cacciari, G. P. Salam, and G. Soyez, *FastJet User Manual*, *Eur. Phys. J.* **C72** (2012) 1896, [[arXiv:1111.6097](#)].
- [77] **DELPHES 3** Collaboration, J. de Favereau, C. Delaere, P. Demin, A. Giammanco, V. Lemaître, A. Mertens, and M. Selvaggi, *DELPHES 3, A modular framework for fast simulation of a generic collider experiment*, *JHEP* **02** (2014) 057, [[arXiv:1307.6346](#)].
- [78] R. Brun and F. Rademakers, *ROOT: An object oriented data analysis framework*, *Nucl. Instrum. Meth.* **A389** (1997) 81–86.
- [79] M. Bahr et al., *Herwig++ Physics and Manual*, *Eur. Phys. J.* **C58** (2008) 639–707, [[arXiv:0803.0883](#)].
- [80] **CMS** Collaboration, *A Cambridge-Aachen (C-A) based Jet Algorithm for boosted top-jet tagging*, .
- [81] M. Cacciari, G. P. Salam, and G. Soyez, *The Anti- $k(t)$ jet clustering algorithm*, *JHEP* **04** (2008) 063, [[arXiv:0802.1189](#)].

- [82] **LUX** Collaboration, D. S. Akerib et al., *First results from the LUX dark matter experiment at the Sanford Underground Research Facility*, *Phys. Rev. Lett.* **112** (2014) 091303, [[arXiv:1310.8214](#)].
- [83] M. Chala, F. Kahlhoefer, M. McCullough, G. Nardini, and K. Schmidt-Hoberg, *Constraining Dark Sectors with Monojets and Dijets*, *JHEP* **07** (2015) 089, [[arXiv:1503.05916](#)].
- [84] F. Kahlhoefer, K. Schmidt-Hoberg, T. Schwetz, and S. Vogl, *Implications of unitarity and gauge invariance for simplified dark matter models*, [arXiv:1510.02110](#).
- [85] M. Garny, A. Ibarra, and S. Vogl, *Antiproton constraints on dark matter annihilations from internal electroweak bremsstrahlung*, *JCAP* **1107** (2011) 028, [[arXiv:1105.5367](#)].
- [86] D. Binosi and L. Theussl, *JaxoDraw: A Graphical user interface for drawing Feynman diagrams*, *Comput. Phys. Commun.* **161** (2004) 76–86, [[hep-ph/0309015](#)].